Inorg. Chem. **2008**, *47*, 9431−9438

Synthesis, Crystal Structures, and Luminescence of Organic-Lanthanide Complexes with Nicotinate and Isonicotinate Ligands

Guohua Jia,[†] Ga-Lai Law,[‡] Ka-Leung Wong,[†] Peter A. Tanner,*[,†] and Wing-Tak Wong[‡]

Department of Biology and Chemistry, City University of Hong Kong, Tat Chee Avenue, Kowloon, Hong Kong S.A.R., P.R. China, and Department of Chemistry, The University of Hong Kong, Pokfulam, Hong Kong S.A.R., P.R. China

Received June 2, 2008

Six lanthanide coordination compounds with two isomeric carboxylic acids, nicotinic acid (H**L**[1]) and isonicotinic acid (H**L**[2]), $[(\mathbf{L}^1)_3Ln(H_2O)_2]_2$ (Ln = Eu, **1**; Gd, **2**; Tb, **3**) and $[(\mathbf{L}^2)_2Ln(H_2O)_4][NO_3]$ (Ln = Eu, **4**; Gd, **5**; Tb, **6**), have been synthesized and structurally characterized by single-crystal X-ray diffraction. Complexes **1**−**3** are dimeric whereas **4**−**6** are polymeric, all with 8-coordination of Ln^{3+}. The distinction between these lanthanide complexes is readily accomplished from the 10 K high resolution electronic emission spectra. Spectral interpretation is given for the Eu^{3+} complexes **1**, **4**, whereas the spectra of **3** and **6** are more complex. The relationships between spectroscopic and crystallographic site symmetries are discussed. The calculated second rank crystal field strengths of Eu^{3+} in **1** and **4** are intermediate in magnitude.

Introduction

There has been burgeoning interest in the design of efficient luminescent organic lanthanide (Ln^{3+}) complexes for application in different areas such as telecommunications and three-dimensional optical storage, with an emerging interest in producing contrast agents.[1−3] Lanthanide ions are commonly employed for optical purposes because of their narrow and sharp bands and distinguishable long lifetimes.[4−8]

However, lanthanide $4f^N-4f^N$ transitions are Laporte forbidden so that the direct excitation of lanthanide ions is not efficient, [9] and the resulting emissions are weak. Thus, chromophoric sensitization of Ln^{3+} by energy transfer from a ligand antenna has been subjected to numerous theoretical and experimental investigations. Indeed, there has been a dramatic increase in the study of different types of organo-chromophores, especially involving the use of rare earth metal labels in analytical and clinical chemistry.[9−15] The motivation of the present work was initially to extend some recent studies of different antennae using multidentate amide ligands which sensitize $4f^N-4f^N$ luminescence through ligand singlet → $^5D_0$ (Eu) or $^5D_4$ (Tb) energy transfer[16] or through ligand singlet → ligand triplet → $^5D_0$ (Eu) or $^5D_4$ (Tb) transfer.[17−20] However, our main focus soon turned to the structural and spectral differences between the lanthanide ion complexes with the two isomeric acids which we employed.

The structures and coordination properties of nicotinic acid (3-pyridine carboxylic acid) and isonicotinic acid (4-pyridine carboxylic acid) with some lanthanide ions were investigated

* To whom correspondence should be addressed. E-mail: bhtan@cityu.edu.hk.
[†] City University of Hong Kong.
[‡] The University of Hong Kong.

(1) Kido, J.; Okamoto, Y. *Chem. Rev.* **2002**, *102*, 2357.
(2) Marques, N.; Sella, A.; Takats, J. *Chem. Rev.* **2002**, *102*, 2137.
(3) Karfeld, L. S.; Bull, S. R.; Davis, N. E.; Meade, T. J.; Barron, A. E. *Bioconjugate Chem.* **2007**, *18*, 1697.
(4) Lemmetyinen, H.; Vuorimaa, E.; Jutila, A.; Mukkala, V.-M.; Takalo, H.; Kankare, J. *Luminescence* **2000**, *15*, 341.
(5) Hebbink, G. A.; Reinhoudt, D. N.; van Veggel, F. C. J. M. *Eur. J. Org. Chem.* **2001**, *21*, 4101.
(6) Fricker, S. P. *Chem. Soc. Rev.* **2006**, *35*, 524.
(7) de Lill, D. T.; Cahill, C. L. *Chem. Commun.* **2006**, *47*, 4946.
(8) Albrecht, M.; Osetska, O.; Klankermayer, J.; Fröhlich, R.; Gumy, F.; Bünzli, J.-C. G. *Chem. Commun.* **2007**, *18*, 1834.
(9) Parker, D. *Chem. Soc. Rev.* **2004**, *33*, 156.
(10) Nitz, M.; Franz, K. J.; Maglathlin, R. L.; Imperiali, B. *ChemBioChem* **2003**, *4*, 272.
(11) Girginova, P. I.; Almeida Paz, F. A.; Soares-Santos, P. C. R.; Ferreira, R. A. S.; Carlos, L. D.; Amaral, V. S.; Klinowski, J.; Nogueira, H. I. S.; Trindade, T. *Eur. J. Inorg. Chem.* **2007**, *26*, 4238.
(12) Su, X.-C.; Huber, T.; Dixon, N. E.; Otting, G. *ChemBioChem.* **2006**, *7*, 1599.
(13) Petoud, S.; Muller, G.; Moore, E. G.; Xu, J.; Sokolnicki, J.; Riehl, J. P.; Le, U. N.; Cohen, S. M.; Raymond, K. N. *J. Am. Chem. Soc.* **2007**, *129*, 77.
(14) Franz, K. J.; Nitz, M.; Imperiali, B. *ChemBioChem* **2003**, *4*, 265.
(15) Bünzli, J.-C. G.; Piguet, C. *Chem. Soc. Rev.* **2005**, *12*, 1048.
(16) Yang, C.; Fu, L.-M.; Wang, Y.; Zhang, J.-P.; Wong, W.-T.; Ai, X.-C.; Qiao, Y.-F.; Zou, B.-S.; Gui, L.-L. *Angew. Chem., Int. Ed.* **2004**, *43*, 5010.

10.1021/ic8010103 CCC: $40.75
Published on Web 09/19/2008

during the 1970s.[21−26] Moore et al.[26] have described the crystal structures of the hydrated lanthanide nicotinates ($\mathbf{L}^1$; Ln = La, Sm) which comprise dimeric units related by an inversion center. Kay et al.[25] determined the crystal structure of the neutral complex of the isonicotinate ion with lanthanum(III): La($\mathbf{L}^2$)$_3$(H_2O)$_2$. Several studies in Russian and not available to us,[21−24] have also concerned complexes of $\mathbf{L}^1$ and $\mathbf{L}^2$ with lanthanide ions. Whereas our study focuses upon the 3- and 4-pyridine carboxylic acids, the crystal structures of the natural chelator 2-pyridine carboxylic acid (picolinic acid) with lanthanide complexes have been reported[27,28] and differ from the complexes with $\mathbf{L}^1$ and $\mathbf{L}^2$ in that nitrogen is able to coordinate to the lanthanide ion. Some other works have been concerned with the crystal structures of complexes of nicotinic and isonicotinic *N*-oxides.[29,30]

In this work, we have sought to investigate the crystal structures of the lanthanide(III) complexes with $\mathbf{L}^1$ and $\mathbf{L}^2$, to distinguish them by spectroscopic methods, and to fully interpret their luminescence spectra. Herein, six organolanthanide complexes with $\mathbf{L}^1$, [Ln($OOCC_5H_4N$)$_3$(H_2O)$_2$]$_2$, Ln = Eu (**1**), Gd (**2**), Tb (**3**), and $\mathbf{L}^2$, [Ln($OOCC_5H_4N$)$_2$(H_2O)$_4$]$^+$[NO_3]$^-$, Ln = Eu (**4**), Gd (**5**), Tb (**6**), were formed by self-assembly with the corresponding acid (Figure 1). The crystal structures of complexes **1** and **3** demonstrate that they are isostructural, as are **4** and **6**. The crystallographic and physicochemical differences between the two pairs are intriguing and are highlighted. Although X-ray data were not obtained for the Gd^{3+} complexes **2** and **5**, analytical data and FTIR spectra show that they are isostructural with **1**, **3** and **4**, **6**, respectively.

Experimental Section

Photophysical Measurements. All solvents were purified and dried by standard methods prior to use.[31] Chemicals, unless otherwise stated, were purchased commercially and used as received. Emission spectra with a resolution of 2−4 cm^{-1} were recorded using an air-cooled Omnichrome Ar^+ laser, or a Panther optical parametric oscillator (OPO) system pumped by the second harmonic of a Surelite Nd^{3+}:YAG laser. The samples were mounted in an Oxford Instruments closed cycle cryostat, with base temperature 10 K. The emission was collected through a 0.5 m Acton spectrometer equipped with a SpectruMM CCD detector.

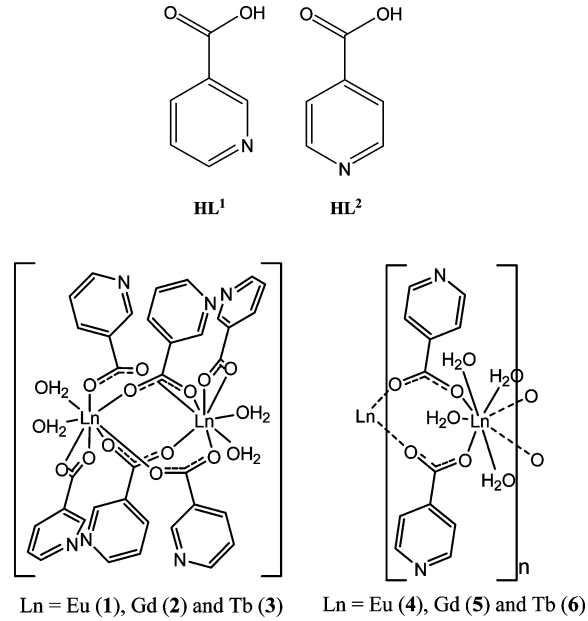

Figure 1. Molecular structures of the acids H$\mathbf{L}^1$, H$\mathbf{L}^2$ (upper), and their lanthanide complexes **1**−**6** (lower).

Synthesis of Lanthanide Complexes 1−3. Nicotinic acid (500 mg, 4.06 × 10^{-3} mol) was used as the chelating ligand with lanthanide nitrate salts Ln(NO_3)$_3$·6H_2O (Ln = Eu (**1**) 1.35 × 10^{-3} mol (632 mg), Gd (**2**) 1.35 × 10^{-3} mol (612 mg), and Tb (**3**) 1.35 × 10^{-3} mol (614 mg)), and the purified product was isolated as a white powder; yield: Eu 71%, Gd 88%, and Tb 77%.

Crystal data for complex **1**, [Eu($OOCC_5H_4N$)$_3$(H_2O)$_2$]: $C_{36}H_{32}N_6O_{16}Eu_2$, M = 1108.6, monoclinic, $P2_1/c$, a = 9.6436(13) Å, b = 11.714(2) Å, c = 17.708(2) Å, β = 91.868(2)°, V = 1999.4(5) Å^3, T = 301 K, Z = 2, μ(Mo Kα) = 31.812 cm^{-1}, 11823 reflections measured, 4372 unique (R_{int} = 0.035), 4022 observed reflections [$I > 2\sigma(I)$] were used in all of the calculations. F to R = 0.023 R_w = 0.028. CCDC: 661889. Anal. **1**: Found: C, 39.02; H, 2.96; N, 7.60. Calcd for $C_{36}H_{32}N_6O_{16}Eu_2$: C, 39.00; H, 2.91; N, 7.58. FAB MS: 1110.

Anal. **2**: Found: C, 38.68; H, 2.91; N, 7.53. Calcd for $C_{36}H_{32}N_6O_{16}Gd_2$: C, 38.63; H, 2.88; N, 7.51. FAB MS: 1119.

Crystal data for complex **3**, [Tb($OOCC_5H_4N$)$_3$(H_2O)$_2$]: $C_{36}H_{32}N_6O_{16}Tb_2$, M = 1122.53, monoclinic, $P2_1/c$, a = 9.636(2) Å, b = 11.704(2) Å, c = 17.702(4) Å, β = 91.857(4)°, V = 1995.4(7) Å^3, T = 301 K, Z = 2, μ(Mo Kα) = 27.50 cm^{-1}, 12115 reflections measured, 4499 unique (R_{int} = 0.040), 3871 observed reflections [$I > 2\sigma(I)$] were used in all of the calculations. F to R = 0.035, R_w = 0.041. CCDC: 661888. Anal. **3**: Found: C, 38.51; H, 2.82; N, 7.43. Calcd for $C_{36}H_{32}N_6O_{16}Tb_2$: C, 38.52; H, 2.87; N, 7.49. FAB MS: 1122.

Synthesis of Lanthanide Complexes 4−6. Isonicotinic acid (500 mg, 4.06 × 10^{-3} mol) was used as the chelating ligand with lanthanide nitrate salts Ln(NO_3)$_3$·6H_2O (Ln = Eu (**4**) 1.35 × 10^{-3} mol (632 mg), Gd (**5**) 1.35 × 10^{-3} mol (612 mg), and Tb (**6**) 1.35 × 10^{-3} mol (614 mg)), and the purified product was isolated as a white powder; yield: Eu 73%, Gd 80%, and Tb 75%.

Crystal data for complex **4**, [Eu($OOCC_5H_4N$)$_2$(H_2O)$_4$]$^+$[NO_3]$^-$: $C_{12}H_{16}N_3O_{11}Eu$, M = 530.23, monoclinic, $C2/c$ (#15), a = 9.2300(9) Å, b = 19.826(2) Å, c = 10.0958(10) Å, β = 108.959(2)°, V = 1747.2(3) Å^3, T = 301 K, Z = 4, μ(Mo Kα)

(17) Law, G.-L.; Kwok, W.-M.; Wong, W.-T.; Wong, K.-L.; Tanner, P. A. *J. Phys. Chem. B* **2007**, *111*, 10858.
(18) Wong, K.-L.; Law, G.-L.; Kwok, W.-M.; Wong, W.-T.; Phillips, D. L. *Angew. Chem., Int. Ed.* **2005**, *44*, 3436.
(19) Wong, K.-L.; Kwok, W.-M.; Wong, W.-T.; Phillips, D. L.; Cheah, K. W. *Angew. Chem., Int. Ed.* **2004**, *43*, 4659.
(20) Luo, L.; Lai, W. P.-W.; Wong, K.-L.; Wong, W.-T.; Li, K.-F.; Cheah, K.-W. *Chem. Phys. Lett.* **2004**, *398*, 372.
(21) Abdul'minev, I. K.; Aslanov, L. A.; Koshits, M. A.; Chupakhina, R. A. *Zh. Strukt. Khim.* **1973**, *14*, 383.
(22) Aslanov, L. A.; Abdul'minev, I. K.; Porai-Koshits, M. A. *Zh. Strukt. Khim.* **1972**, *13*, 468.
(23) Aslanov, L. A.; Kiekbaev, I. D.; Abdul'minev, I. K.; Porai-Koshits, M. A. *Kristallografiya* **1974**, *19*, 179.
(24) Aslanov, L. A.; Kiekbaev, I. D.; Abdul'minev, I. K.; Porai-Koshits, M. A. *Kristallografiya* **1974**, *19*, 170.
(25) Kay, J.; Moore, J. W.; Glick, M. D. *Inorg. Chem.* **1972**, *11*, 2818.
(26) Moore, J. W.; Glick, M. D.; Baker, J. W., Jr. *J. Am. Chem. Soc.* **1972**, *94*, 1858.
(27) Ma, J.-F.; Jin, Z.-S.; Ni, J.-Z. *Polyhedron* **1995**, *14*, 563.
(28) Ma, J.-F.; Hu, N.-H.; Ni, J.-Z. *Polyhedron* **1996**, *15*, 1797.
(29) Mao, J.-G.; Zhang, H.-J.; Ni, J.-Z.; Wang, S.-B.; Mak, T. C. W. *Polyhedron* **1998**, *17*, 3999.
(30) Goher, M. A. S.; Mautner, F. A. *J. Mol. Struct.* **2007**, *846*, 153.
(31) Perrin, D. D. Armarego, W. L. F. *Purification of Laboratory Chemicals*, 4th ed.; Pergamon: Oxford, 1996.

= 36.47 cm^{-1}, 5345 reflections measured, 1950 unique (R_{int} = 0.021), 1813 observed reflections [$I > 2\sigma(I)$] were used in all of the calculations. F to R = 0.021, R_w = 0.025. CCDC: 661886. Anal. **4**: Found: C, 27.20; H, 3.03; N, 7.89. Calcd for $C_{12}H_{16}N_3O_{11}Eu$: C, 27.18; H, 3.04; N, 7.92. FAB MS: 531.

Anal. **5**: Found: C, 30.48; H, 3.40; N, 5.98. Calcd for $C_{12}H_{16}N_2O_8Gd$: C, 30.44; H, 3.41; N, 5.92. FAB MS: 536.

Crystal data for complex **6**, $[Tb(OOCC_5H_4N)_2(H_2O)_4]^+[NO_3]^-$: $C_{12}H_{16}N_3O_{11}Tb$, M = 537.20, monoclinic, $C2/c$ (#15), a = 9.2127(8) Å, b = 19.803(2) Å, c = 10.0537(9) Å, β = 108.980(2)°, V = 1734.5(3) $Å^3$, T = 301 K, Z = 4, μ(Mo Kα) = 41.34 cm^{-1}, 5267 reflections measured, 1931 unique (R_{int} = 0.020), 1873 observed reflections [$I > 2\sigma(I)$] were used in all of the calculations. F to R = 0.019, R_w = 0.024. CCDC: 661887. Anal. **6**: Found: C, 26.87; H, 3.01; N, 7.89. Calcd for $C_{12}H_{16}N_3O_{11}Tb$: C, 26.83; H, 3.00; N, 7.82. FAB MS: 538.

Crystallography. Single crystals suitable for X-ray crystallographic analyses for complexes **1**, **3**, **4**, and **6** were mounted in glass capillaries. Diffraction data were collected at room temperature on a Bruker AXS SMART 1000 CCD diffractometer equipped with graphite-monochromated Mo Kα radiation (λ = 0.71073 Å). Intensity data were also corrected for Lorentz and polarization effects, and an approximation of absorption correction by inter-image scaling was applied. The space groups of both crystals were determined from a combination of Laue symmetry checks, and their systematic absences were confirmed by successful refinement of the structures. The structures were solved by direct methods, SIR 92, [32] or SHELXS97,[33] along with Fourier-difference techniques. Structural refinements were made on F by full-matrix least-squares analysis. The hydrogen atoms of the organic moieties were generated in their idealized positions. All calculations were performed on a PC computer using the program package CrystalStructure.[34]

Results and Discussion

Crystal Structures of 1, 3, 4, and 6. Complexes **1**−**6** are formed by mixing nicotinic or isonicotinic acid with the appropriate lanthanide nitrate salts. The products were recrystallized in methanol for X-ray and photophysical studies.

Complexes **1** and **3** are both dimeric. Each lanthanide ion is 8-coordinate with all eight Ln−O distances different. Although the nicotinic acids are coordinated to lanthanide ions solely through carboxylate groups, there are two types of bonding mode: four bridging bidentate and one chelating bidentate, which account for six coordination sites. The first coordination spheres of the lanthanide ions are completed by two aqua ligands. The dimeric lanthanide complex is thus a neutral entity, with the two trivalent charges of Ln^{3+} balanced by the six nicotinate anions, $[Ln_2(\mu\text{-}OOCC_5H_4N)_4(OOCC_5H_4N)_2(H_2O)_4]$. There is an inversion center situated at the midpoint of the two Ln centers in the dimer. The structure and packing diagram of **1** and **3** are shown in Figure 2. The metal−metal distances are 4.3607(3) Å (Tb−Tb) and 4.3629(1) Å (Eu−Eu). The complexes **1** and **3** are isostructural with the La and Sm complexes described by Moore et al.[26]

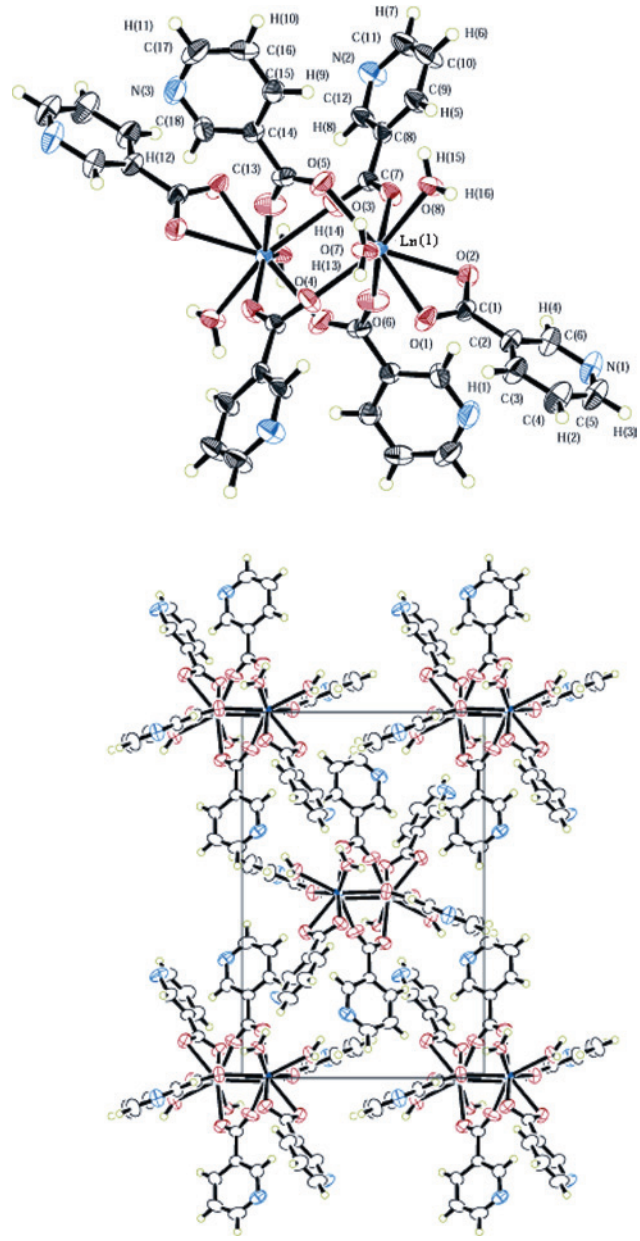

Figure 2. Oak Ridge Thermal Ellipsoid Plot (ORTEP) drawing and packing diagram of nicotinate complexes **1** and **3** (**1**: Ln = Eu, **3**: Ln = Tb).

The carboxylate oxygen-lanthanide distances range from 2.339(3) Å to 2.542(2) Å for **1** and 2.336(5) Å to 2.534(4) Å for **3** (Supporting Information, Table S1) with an average value of 2.409 Å for **1** and 2.406 Å for **3**. The two aqua oxygens have an average bonding distance of 2.407 Å (Eu) and 2.412 Å (Tb). It is interesting to find that the Ln−O(bridging) distances are comparatively shorter (∼0.2 Å) than the Ln−O(chelating) distance. This may be due to the fact that in bidentate chelating mode the small bite angle O(1)−Ln(1)−O(2) ∼51.7° in **1** and **3** at Ln weakens the Ln···O bonding interactions. The coordination polyhedron is a slightly distorted bicapped trigonal prism, or it has been

(32) SIR 92. Altomare, A.; Cascarano, G.; Giacovazzo, C.; Guagliardi, A.; Brula, M. C.; Polidori, G.; Camalli, M. *J. Appl. Crystallogr.* **1994**, *27*, 435.
(33) Sheldrick, G. M. *SHELXS 97*; University of Göttingen: Göttingen, Germany, 1997.
(34) (a) *CrystalStructure. Single Crystal Structure Analysis Software*, version 3.5.1; Rigaku/MSC Corporation: The Woodlands, TX, 2003. (b) Watkin, D. J.; Prout, C. K.; Carruthers, J. R; Betteridge, P. W. *Crystals*; Chemical Crystallography Lab.: Oxford, U.K., 1996; Issue 10.

described by Moore et al.[26] as a highly distorted square antiprism. The top isosceles triangle is formed by O(3), O(5), and O(8), with the congruent angles of about 60.8°, and ∠O(3)O(8)O(5) is 58.5°. The bottom isosceles triangle is formed by O(1), O(4), and O(6), with the congruent angles of ~ 64.4° and ∠O(4)O(1)O(6) 51.1°. The dihedral angle between the top and the bottom planes is 12.50°.

A plot of mean Ln−O distance versus atomic number for $[Ln(OOCC_5H_4N)_3(H_2O)_2]_2$ decreases in a perfectly linear manner for Ln = La,[26] Sm,[26] and Tb but the mean Eu−O distance is 0.04 Å longer than the extrapolation of this line, showing that steric constraints limit a further bond distance shortening.

In the nicotinate ligands, the pyridyl rings are not always coplanar with the carboxylate groups and the twisting angle ranges between 5.63 and 21.67°. It is interesting to find that there are no significant $\pi\cdots\pi$ or C−H$\cdots\pi$ interactions found. However, there is extensive strong intermolecular O−H···N or O−H···O and weak C−H···O−H bonding in the crystal lattice (see Supporting Information, Table S2).

It is interesting to compare the coordination geometry of **1** and **3** with that of Ln = Eu, Tb in $[Ln(\mathbf{L}^1O)_3(H_2O)_2]_n\cdot 4H_2O$[29] ($H\mathbf{L}^1O$ is nicotinic acid *N*-oxide) where the carboxylate groups are involved in three different coordination modes (chelating, bridging and unidentate) and the N−O group completes the 8-coordination of Ln^{3+}. Again, the Ln−O (bridging) distances are smaller than Ln−O (chelating). However, the Ln−O (unidentate) distances are smallest.

Complexes **4** and **6** exist as polymers running parallel to the *c*-axis. Each 8-coordinate lanthanide ion is coordinated to four oxygens from four bridging isonicotinate ligands and four oxygens from four aqua ligands. The structure drawing and packing diagram of **4** and **6** are shown in Figure 3. Metal−oxygen bond distances are listed in Supporting Information, Table S3. These distances are rather longer for **4** (mean value 2.419 Å) than for **6** (mean value 2.392 Å). The complex has a unipositive charge which is counterbalanced by a nitrate anion situated between the polymeric $[M(\mathbf{L}^2)_2(H_2O)_4]$ chains. Each Ln^{3+} center has a distorted/pseudo square antiprism geometry, with O(1)/O(2)^i/O(3)^i/O(4) as the top plane (max. deviation of 0.219 Å from the mean plane) and the O(1)^i/O(2)/O(3)/O(4)^i as the bottom plane for Eu, **4** (i: $-x$, y, $^1/_2 - z$); while O(1)/O(2)^i/O(3)^i/O(4)^i as the top plane (max. deviation of 0.218 Å from the mean plane) with O(1)^i/O(2)/O(3)/O(4) as the bottom plane for Tb, **6** (i: $1 - x$, y, $^1/_2 - z$). The dihedral angle between the two planes is 2.7° (for **4**) or 2.62° (for **6**). The Ln^{3+} ion is 1.303 Å (**4**) or 1.291 Å (**6**) from either plane. The pyridyl planes in the isonicotinate ligand are not coplanar with the carboxylate group, with the dihedral angles between the two planes being 12.41° (Eu, **4**) or 12.65° (Tb, **6**). By contrast to the nicotinate dimer analogue which has no $\pi\cdots\pi$ or C−H$\cdots\pi$ interactions, there exist both intra- and interpolymer chain $\pi\cdots\pi$ interactions: the intrachain plane-to-plane distance of the pyridyl rings is 3.363 Å (Eu, **4**) or 3.365 Å (Tb, **6**); and the interchain plane-to-plane distance is 3.243 Å (Eu, **4**) or 3.234 Å (Tb, **6**). The extensive intra- and

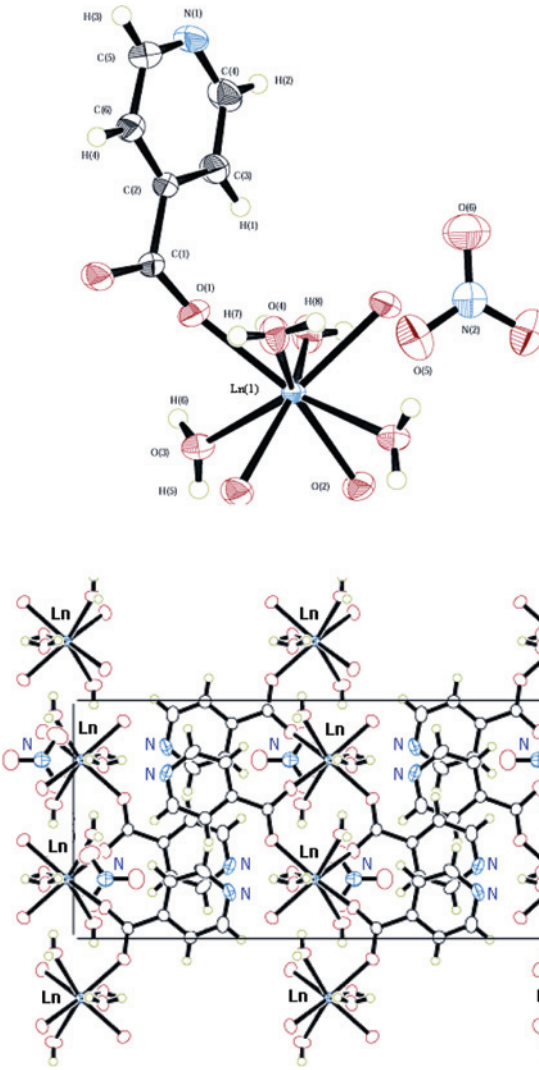

Figure 3. ORTEP drawing and packing diagram of isonicotinate complexes **4** and **6** (**4**: Ln = Eu, **6**: Ln = Tb).

intermolecular hydrogen bonding (Supporting Information, Table S4) connects the ionic-polymeric chain and the anions into a 3-D network. Note that a major difference between pairs **4**, **6**, and **1**, **3** is the much weaker metal−metal interaction in the latter pair, with Ln−Ln distances within the polymers being 5.06 ± 0.02 Å for **4 and 6**.

Again, it is interesting to compare the structures of **4** and **6** with those from lanthanide complexes with isonicotinic acid *N*-oxide ($H\mathbf{L}^2O$) ($[\{Ln(\mathbf{L}^2O)_2(H_2O)_4\}_n](NO_3)_n\cdot nH_2O$[29,30]) where there is no $\mathbf{L}^2O$ coordination to Ln^{3+} via N−O, and the 8-coordination comprises four aqua ligands with the carboxylate groups only being involved in the *syn-syn* bridging mode. Just as in **4** and **6**, the nitrate groups are not involved in coordination to Ln^{3+}.

Photophysical Properties of Complexes 1−6. The IR spectra of $H\mathbf{L}^1$ and $H\mathbf{L}^2$ exhibit an intense broad band at 1710 cm^{-1} due to C═O stretching. The IR spectra of **1** and **4** are very similar. In these complexes the carboxylic acid mode moves to 1589 cm^{-1} (antisymmetric COO^- stretch) and 1416 cm^{-1} (symmetric COO^- stretch). A sharper band at 1545 cm^{-1} is due to the aromatic ring stretch. Other prominent bands are at 765, 713, and 684 cm^{-1}.

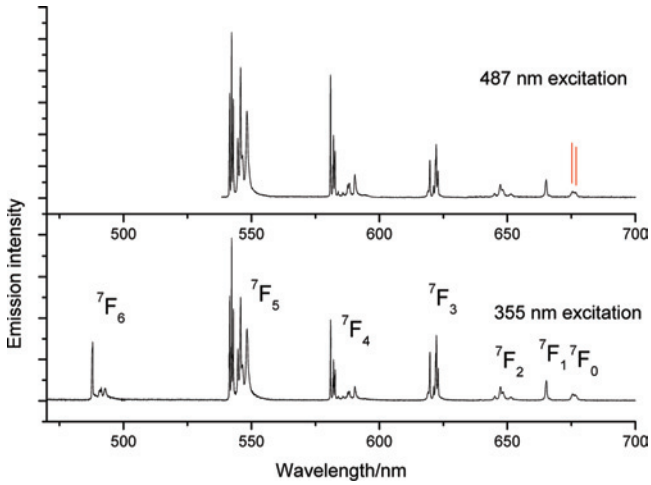

Figure 4. Survey 10 K emission spectra of Tb^{3+} complex **6** using 487 and 355 nm excitation from 470 to 700 nm. The terminal multiplet terms of ^7F_J are marked. The $^5D_4 \rightarrow {}^7F_6$ transition was not recorded for 487 nm excitation.

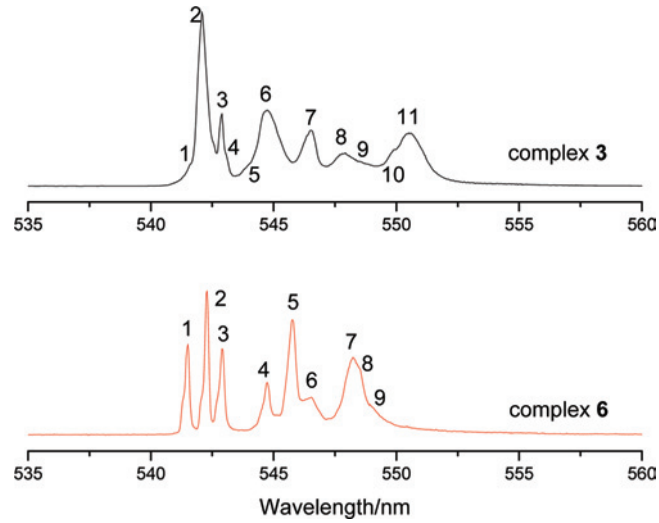

Figure 5. Emission spectra at 10 K of Tb^{3+} complex **3** (excited by 355 nm radiation) and **6** (excited by 488 nm radiation) between 535 to 560 nm showing the $^5D_4 \rightarrow {}^7F_5$ transition. Refer to the text for the band numbering.

The room temperature $4f^N$ emission spectra of **1**, **3**, **4**, and **6** under 300 nm excitation are readily assigned. For complexes **4** and **6**, four structured narrow visible emission bands at 480, 545, 580, 620 nm of Tb^{3+} are assigned to an electronic transitions $^5D_4 \rightarrow {}^7F_J$ (J = 6, 5, 4, 3), whereas bands at 594, 620, 650, 700 nm of Eu^{3+} complexes **1** and **3** correspond to $^5D_0 \rightarrow {}^7F_J$ (J = 1, 2, 3, 4).

Figure 4 shows the survey emission spectra of complex **6** at 10 K under two different laser excitation lines. The purpose of testing the excitation line dependence is to verify the absence of features due impurity species which were present before recrystallization. In fact the two spectra are very similar (as well as for other excitation lines employed) except for enhancement of hot bands under 355 nm excitation (this detail is not visible in the survey spectrum) because of the higher laser power employed. The transitions are readily assigned to emission from the $^5D_4$ multiplet to ^7F_J (J = 6,...,0). The $^5D_4$ lowest levels are at 20511 and 20505 cm^{-1}, so that where resolved, the hot bands are at 6 cm^{-1} to high energy of spectral features. The assignment of the terminal multiplet terms is straightforward in Figure 4.

The site symmetry of the lanthanide ion is C_1 in each of the complexes **1**−**3** and C_2 for **4**−**6**, and there is only one type of lanthanide ion in the unit cell. However, it is not straightforward to assign the crystal field levels of Tb^{3+} in the complexes **3** and **6** for several reasons which are illustrated in Figure 5, where the more detailed $^5D_4 \rightarrow {}^7F_5$ spectra of **3** and **6** are presented. First, at the measurement temperature of 10 K, bands have a splitting of 6 cm^{-1} for **6** (and of 7 cm^{-1} for **3**) due to two emissive states, which is only partially, or not completely resolved in some cases. The measurement of band energies is therefore inaccurate. All crystal field level degeneracies are removed for Tb^{3+} at the C_1 site so that the transition in Figure 5 for **3** should comprise $2J + 1 = 11$ bands. Although it is possible, with some imagination, to count 11 bands for **3**, as marked in the figure, assuming that they all correspond to pure electronic transitions, this is not the case for complex **6** where fewer bands are observed. Some of the derived crystal field splittings for **3** and **6** are similar but the band intensities are very different. This emphasizes the sensitivity of Tb^{3+} to its coordination environment via low temperature electronic spectra, even though the $4f^8$ electrons are inner, shielded electrons. With such complexes having large vibrational degrees of freedom, some electronic energy levels may be perturbed because of electron−phonon couplings. For example, this appears to be the case for the $^5D_4 \rightarrow {}^7F_0$ band which should be a singlet, whereas two features separated by 29 cm^{-1} are resolved, as marked by two vertical lines in the upper spectrum of Figure 4. In this case the resonance occurs between an electronic and a vibronic transition, and there are several possible assignments which could be put forward for the nature of the vibration which are not discussed here. The vibronic bands are otherwise weak, or overlap other pure electronic bands, in the luminescence spectra of **3** and **6**. The clearest observations concern very weak features to low energy of the $^5D_4 \rightarrow {}^7F_6$ transition (not apparent in Figure 4), where the bands are observed at vibrational displacements of 1416 cm^{-1} and 1589 cm^{-1}, which correspond to the energies of IR bands described above.

It is more instructive to consider the low temperature emission spectra of the Eu^{3+} complexes because the higher energy transitions from the nondegenerate $^5D_0$ level are particularly simple. The 10 K luminescence spectra of **1** and **4** were recorded in the region between 19000 cm^{-1} and 14140 cm^{-1} using various excitation lines into $^5D_2$. The 10 K survey spectrum of **1** under 465 nm excitation is shown in Figure 6. Weak emission is observed from $^5D_1$ to terminal multiplets, $^5D_1 \rightarrow {}^7F_{J'}$ (marked as J' in the figure) and the stronger bands represent the emission from $^5D_0$ (marked as J according to the terminal ^7F_J multiplet term label). In the expansion (upper) spectrum of Figure 6, some bands are marked which correspond to vibronic transitions of $^5D_0 \rightarrow {}^7F_2$ crystal field levels involving 1416 cm^{-1} (marked as a in Figure 6) and 1589 cm^{-1} (marked as b) carboxylic acid

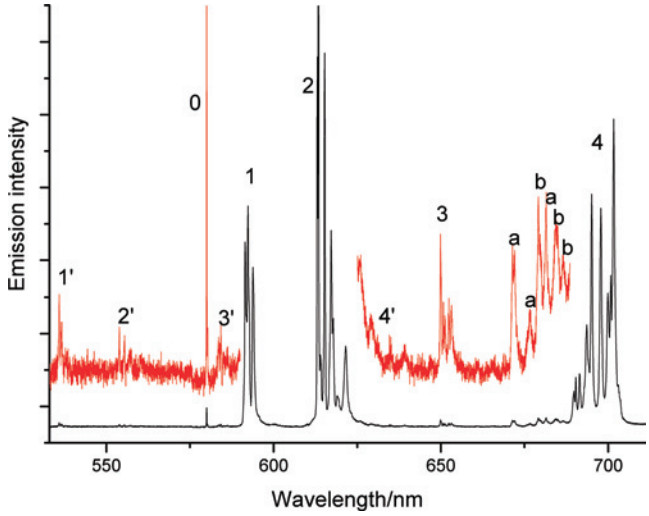

Figure 6. Survey 10 K emission spectrum of **1** under 465 nm excitation. The upper spectrum shows an intensity scale expansion. The terminal J' (J) levels of ^7F_J are marked for transitions from $^5D_1$ ($^5D_0$), respectively. Refer to the text for the explanation of the vibronic structures a and b of $^5D_0 \rightarrow {}^7F_2$.

modes. These vibrations appear strongest when based upon this hypersensitive transition $^5D_0 \rightarrow {}^7F_2$.

The detailed structures in the $^5D_0 \rightarrow {}^7F_1$, $^7F_2$ regions of 10 K emission spectra of **1** and **4** are shown in Figure 7 under various excitation lines. The intrinsic emissions are distinguished from impurity bands (which show remarkable excitation line-intensity dependence) and are numbered for these two transitions. For each complex, the $^5D_0 \rightarrow {}^7F_0$ electronic origin is very weak and is situated at 17233 cm^{-1} for **1** and at 17241 cm^{-1} for **4**. First, we focus upon the spectral interpretation of **1** in Figure 7. Three similar, strong bands (labeled 1−3) are observed for the $^5D_0 \rightarrow {}^7F_1$ transition. The occurrence of both the $^5D_0 \rightarrow {}^7F_0$ transition and of three bands for the $^5D_0 \rightarrow {}^7F_1$ transition in the spectrum of **1** infers that the "spectroscopic" Eu^{3+} site symmetry has a plane or 2-fold axis at most,[35,36] as could be envisaged by slightly readjusting its crystallographically determined geometry to undistorted bicapped trigonal prismatic *(pseudo-C_{2v})* coordination geometry. The derived $^7F_1$ multiplet term crystal field energy levels for **1** are 335, 363, 406 cm^{-1}. For systems with a symmetry plane or axis, the B_1^2 crystal field parameter (Wybourne notation) is zero, and a suitable axis rotation can set imaginary parameters to zero, so that the remaining crystal field parameters are B_0^2 and B_2^2 for ($J = 1$ only B_q^k, $k = 2$ parameters are required to fit the crystal field energy levels in the intermediate coupling approximation since $k \leq 2J$).[36] Neglecting J-mixing, and modeling the energy levels by orthorhombic symmetry, the relevant equations for the energies of the three $^7F_1$ levels are given by[37]

$$E_1 = E_{bar} + 0.2B_0^2 \quad (1)$$

$$E_2 = E_{bar} - 0.1B_0^2 + 0.245B_2^2 \quad (2)$$

$$E_3 = E_{bar} - 0.1B_0^2 - 0.245B_2^2 \quad (3)$$

where the $^7F_1$ barycenter energy, E_{bar}, is the average of the three experimental energies. There are six alternative solutions to these equations for B_0^2, B_2^2 for **1**, but if we consider that lines 1 and 2 are split from a degenerate state, then, $E_{bar} = 368$ cm^{-1}, and from eq 1, $B_0^2 = 190$ cm^{-1}; and substitution into eq 2 gives $B_2^2 = 57$ cm^{-1}. The fitting of $^7F_2$ energy levels require the inclusion of fourth-order crystal field parameters and are not considered here since there is a problem in their assignments because six bands (lines 4−9) are observed instead of the expected 5, most likely because of the presence of vibrational structure.

Turning to the emission spectrum of **4** in Figure 7, although 3 bands (lines 1−3) are observed for $^5D_0 \rightarrow {}^7F_1$ the splitting between lines 2 and 3 is only 5 cm^{-1}. This suggests a slight deviation from an ideal Eu^{3+} site symmetry where the level is degenerate and where a symmetry axis or order n ($n > 2$) is present. In fact, the local environment of

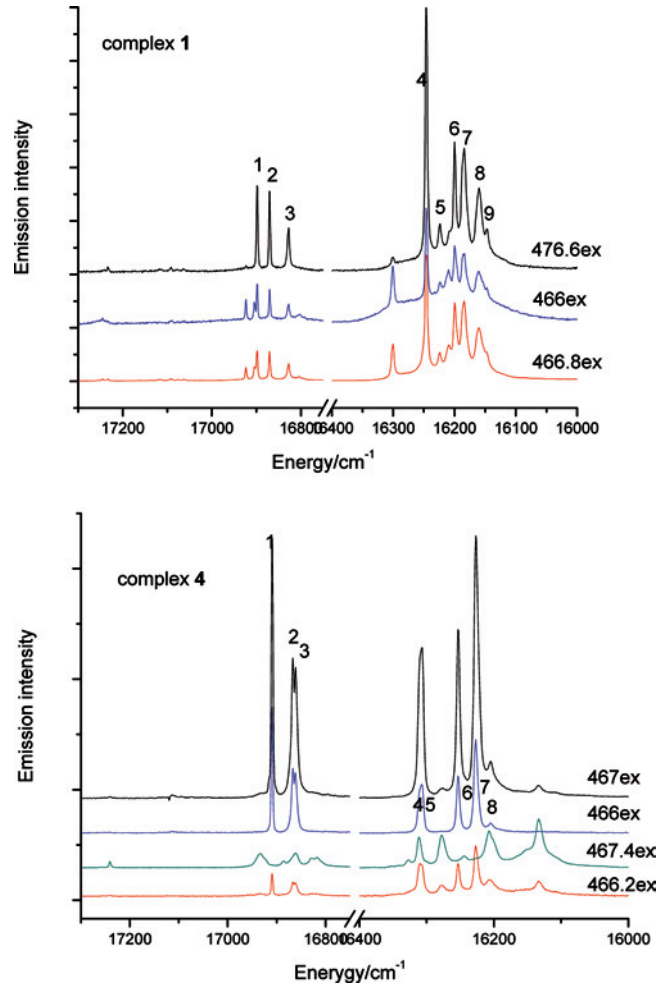

Figure 7. Emission spectra at 10 K between 17300 and 16000 cm^{-1} for **1** and **4** using various laser excitation lines, marked in nm in the figures. Refer to the text for the band numbering.

(35) Chen, X. Y.; Liu, G. K. *J. Solid St. Chem.* **2005**, *178*, 419.
(36) (a) Görller-Walrand, C.; Binnemans, K. *Handbook on Phys. Chem. Rare Earths* **1996**, *23*, 121. (b) (We are indebted to Prof. C. K. Duan for pointing out that $7\sqrt{2}$ in eqs (178) and (179) on page 225 should be $2\sqrt{7}$).
(37) Lavin, B.; Babu, P.; Jayasankar, C. K.; Martin, I. R.; Rodriguez, V. D. *J. Chem. Phys.* **2001**, *115*, 10935.

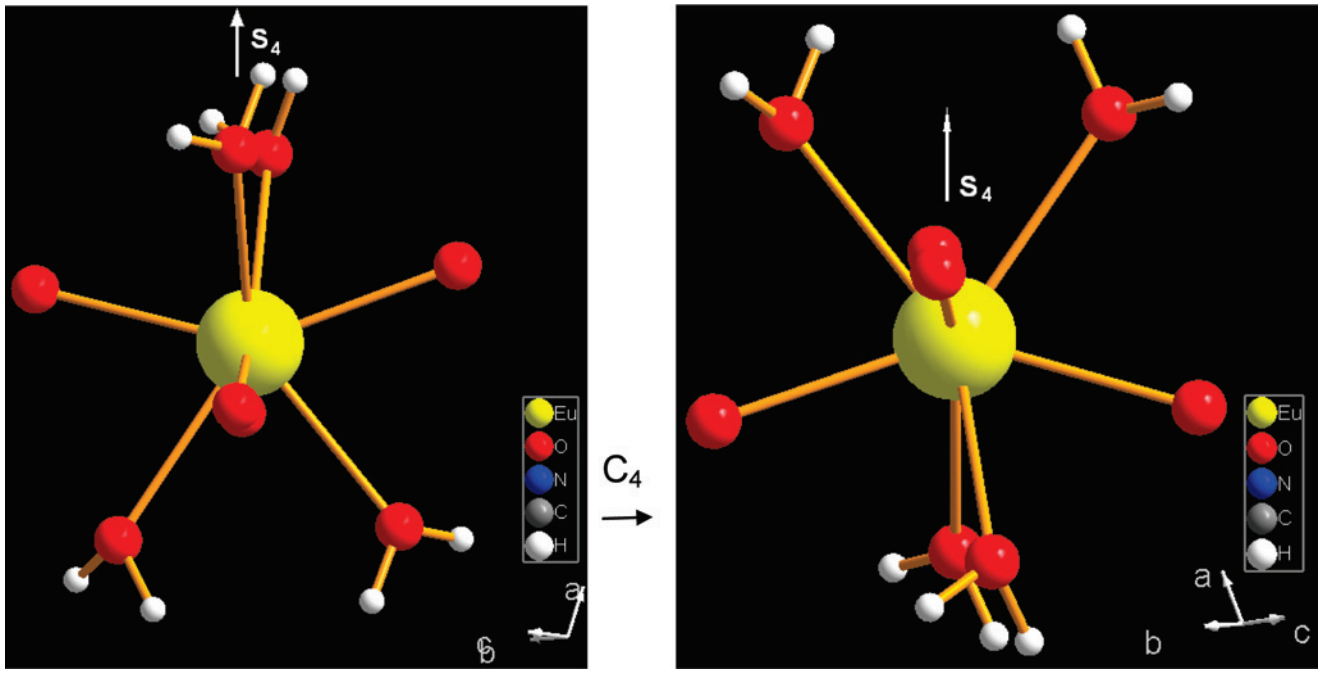

Figure 8. Local coordination environment of Eu^{3+} in **4** showing the location of an approximate S_4 axis and the effect of a 90° rotation about this axis. The distortion of the idealized symmetry plane perpendicular to the S_4 axis is evident from the locations of the four Ln−O (carboxylate) bonds.

Eu^{3+} (as shown in Figure 8) *almost* comprises an S_4 axis. For systems with tetragonal, hexagonal, or trigonal symmetry one of the $^7F_1$ crystal field levels is degenerate so that only two spectral bands are observed for $^5D_0 \rightarrow {}^7F_1$. The presence of S_4 symmetry also implies that only three bands are observed for the $^5D_0 \rightarrow {}^7F_2$ transition, which is almost the case for **4** where three strong features dominate in lines 4−8, Figure 7. It is well-known[38] that the relative positions of the degenerate and nondegenerate $^7F_1$ crystal field levels are determined by the sign of B_0^2. In the present case for **4**, the (almost!) degenerate level is at higher energy (i.e., the transition to it is at lower energy in Figure 7) so that B_0^2 is negative. The value of B_0^2 can be estimated from the correlation between the $^7F_1$ splitting (45 cm^{-1} for **4**) and B_0^2 (Figure 20 in ref 36) to be -169 ± 12 cm^{-1} (where B_2^2 would be zero). More accurately, using eqs 1−3 above, $B_0^2 = -150$ cm^{-1} and $B_2^2 = -8$ cm^{-1}. The small value of B_2^2 emphasizes the small distortion from S_4 symmetry.

The second rank crystal field strength parameter has been defined as[39]

$$N_v(B_q^2) = 1.585[(B_0^2)^2 + 2(B_2^2)^2]^{0.5} \quad (4)$$

and thus for Eu^{3+} equals 327 cm^{-1} for **1** (with the value independent of the symmetry axis chosen) and 238 cm^{-1} for **4**. This is consistent with the fact that the mean Eu−O distance in **1** (2.408 Å) is shorter than that in **4** (2.419 Å). The crystal field strengths fall in the midrange for europium ion systems previously analyzed.[36]

Conclusions

Lanthanide complexes derived from nicotinic acid H**L**[1] and isonicotinic acid H**L**[2] have been synthesized and exhibit dimeric and polymeric structures, respectively, as determined by X-ray crystallography. The low-temperature spectra are well-resolved as shown, for example, by the comparison with the spectra of Eu^{3+} and Tb^{3+} nicotinate complexes covalently linked to a 1,10-phenanthroline functionalized sol−gel glass.[40] The 8-fold coordination geometry of Ln^{3+} in $[Ln(\mathbf{L}^1)_3(H_2O)_2]_2$ (**1**, **3**) and $[Ln(\mathbf{L}^2)_2(H_2O)_4]^+[NO_3]^-$ (**4**, **6**) differs by the presence of four aqua ligands in the latter, whereas eight independent Ln−O carboxylate distances occur for (**1**, **3**). The room temperature solid-state emission spectra of **1**,**4** and **3**,**6** show the characteristic multiplet-multiplet transitions of Eu^{3+} and Tb^{3+}, respectively. The low temperature emission spectra exhibit considerable fine structure although it is necessary to exclude certain bands with variable relative intensities with different laser excitation lines since these are due to other impurity species. Although the Tb^{3+} emission spectra are too complex to merit a simple interpretation, the Eu^{3+} emission spectra can be assigned and interpreted. In fact the spectroscopic data clearly indicate the idealized coordination geometries of Ln^{3+} in **1** and **4** and the presence of slight distortions from these.

Acknowledgment. The financial support of the Hong Kong Research Grants Council Research Grant 102607, the City University of Hong Kong and the University of Hong Kong is acknowledged. G.H.J. acknowledges the receipt of

(38) Binnemans, K.; Görller-Walrand, C. *Chem. Phys. Lett.* **1995**, *245*, 75.
(39) Auzel, F. *Mater. Res. Bull.* **1979**, *14*, 223.
(40) Lenaerts, P.; Görller-Walrand, C.; Binnemans, K. *J. Lumin.* **2006**, *117*, 163.

a postgraduate studentship administered by City University of Hong Kong, and K.L.W. acknowledges the Research Scholarship Enhancement Scheme of City University of Hong Kong.

Supporting Information Available: Tables S1−S4: selected bond lengths, bond angles and hydrogen-bonding geometry of **1**−**6**. This material is available free of charge via the Internet at http://pubs.acs.org. Crystallographic information for **1**, **3**, **4**, and **6** is available free of charge as CIF records CCDC 661886 to 661889 inclusive from the Cambridge Crystallographic Data Centre (CCDC) via the web link www.ccdc.cam.ac.uk/data_request/cif.

IC8010103